Post-buckling and Snap-Through Behavior of Inclined Slender Beams

Jian Zhao

Jianyuan Jia

School of Elec-mechanical Engineering,
Xidian University,
Xi'an, 710071, P.R.C.

Xiaoping He
Institute of Electronic Engineering,
China Academy of Engineering Physics,
Mianyang 621900, P.R.C.

Hongxi Wang
School of Elec-mechanical Engineering,
Xidian University,
Xi'an, 710071, P.R.C.

Based on the geometrical nonlinear theory of large deflection elastic beams, the governing differential equations of post-buckling behavior of clamped-clamped inclined beams subjected to combined forces are established. By using the implicit compatibility conditions to solve the nonlinear statically indeterminate problems of elastic beams, the strongly nonlinear equations formulated in terms of elliptic integrals are directly solved in the numerical sense. When the applied force exceeds the critical value, the numerical simulation shows that the inclined beam snaps to the other equilibrium position automatically. It is in the snap-through process that the accurate configurations of the post-buckling inclined beam with different angles are presented, and it is found that the nonlinear stiffness decreases as the midpoint displacement is increased according to our systematical analysis of the inward relations of different buckling modes. The numerical results are in good agreement with those obtained in the experiments.
[DOI: 10.1115/1.2870953]

Keywords: geometrical nonlinearity, snap through, nonlinear stiffness, post-buckling, large deflection

1 Introduction

In microelectromechanical system (MEMS) fields, a need arises in engineering practice to predict accurately the nonlinear response of slender post-buckling beams, especially the nonlinear transverse stiffness. The bistability of the post-buckling beams is excellent in reducing power consumption of microdevices or microsystems. However, the major difficulty in analyzing the post-buckling and snap-through response is the intractability of the geometric nonlinear control equations of large deflection beams. Enikov et al. [1] designed a V-shaped thermal microacturator with buckling beams. Yet, the precise computation model for the buckling beam based on the large deflection theory has not been built. Seide [2] discussed the accuracy of some numerical methods for column buckling. Mau [3] studied the stability of the post-buckling paths of columns with discrete spring supports. Though Fang and Wickert [4] studied the static deformation of micromachined beams under in-plane compressive stress, they could not trace the post-buckling paths by making use of the linearized governing differential equation. Wang [5] presented the complete post-buckling and large deformations of an elastica rod, one end fixed and one end pinned. Hartono [6,7] applied the elastica solution to describe the large displacement behavior of a column with lateral bracing at the midheight and obtained the post-buckling configurations of the deformed column under the axial loading. Coffin and Bloom [8] analyzed the post-buckling response of an elastic and hygrothermal beam fully restrained against axial expansion. Li and Zhou [9] studied the post-buckling behavior of a hinge-fixed beam under evenly distributed follower forces. The post-buckling analysis of the easily fabricated MEMS beams with both ends fixed is really important in the design of microstructures. To solve the post-buckling problems of small deformation beams, the predominant approach is to use a nonlinear finite element (FE) model, or to resort to a linear analytical model based on the small deflection theory, which agrees only with experiments in a relatively limited range of loadings. The apex displacement of the bent beam can only be reduced in nearly linear proportion to the vertical force in the design of microactuators [10,11], and the error is large compared with the experimental results. This lack of a simple and yet accurate tool for analyzing the post-buckling bent beams results in a poor initial "guess" of the desired geometry and multidesign iterations, thus being unable to provide an insight into the deformation problems. Therefore, the large deflection buckling theory is needed to solve the intractability of the geometric nonlinear control equations of the bent beam.

Aiming at designing a novel MEMS threshold acceleration switch with post-buckling beams, this paper studies the post-buckling behavior in the snap-through process of the large deflection inclined beam with both ends fixed, and establishes the nonlinear governing equations of the post-buckling beam under combined forces acting on the ending point. These ordinary nonlinear differential equations consist of the boundary-value conditions, in which six unknown functions are contained and the length of the deformed beam is considered as one of the unknown functions. By using the implicit compatibility conditions to express the nonlinear statically indeterminate problems of elastic beams, the strongly nonlinear equations formulated in terms of elliptic integrals are directly solved in the numerical sense. Through an incremental displacement method, we can obtain the equilibrium paths of the deformed beam in the snap-through process, and describe explicitly the nonlinear force-and-displacement relations of the central point of the bent-beam structure. For further applications of the nonlinear stiffness of the post-buckling beams, an electronic testing device is designed. The simulation results are in good agreement with those by experiments.

2 Governing Equations of Post-buckling Beams

2.1 Nonlinear Structure Supported by Inclined Beams. A typical bent-beam structure is shown in Figs. 1 and 2. The structure consists of one inertial mass supported by two inclined beams with length L, both ends fixed. The central mass is constrained to move vertically. When a vertical force F_v is applied on the central node, the constraint beam is subjected to the compression and lateral bending moments, thus resulting in the symmetric response

Contributed by the Applied Mechanics Division of ASME for publication in the JOURNAL OF APPLIED MECHANICS. Manuscript received April 16, 2007; final manuscript received November 9, 2007; published online May 16, 2008. Review conducted by Edmundo Corona.

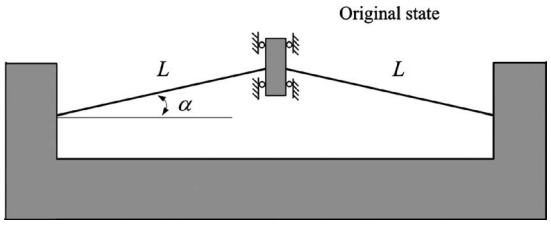

Fig. 1 Original state of the bent-beam structure

of the beam. When the vertical force F_v exceeds the critical buckling load, the inclined beam with initial angle α buckles, and then snaps to the next equilibrium state. During the whole snap-through process, the structural stiffness varies with the displacements of the central node. As we all know, the nonlinear stiffness of the inclined beam plays a crucial role in the action of the nonlinear system; therefore, it is of great importance to study the post-buckling behavior of the inclined beam, which experiences large deflections, and to show the equilibrium paths during the snap-through process.

2.2 Governing Equations of the Post-buckling Beam. Based on the symmetry of the structure, the left half span of the bent beam with reaction forces is analyzed, and the coordinate system used is shown in Fig. 3. When the right ending point of the beam moves vertically, the beam buckles and the configuration becomes asymmetric or symmetric depending on the number of inflection points along the deformed beam. The moment at the inflection point is zero. By using the geometric symmetry, a coordinate system is constructed accordingly. Let a Cartesian coordinate system (x,y) be located at the left fixed end, and s stands for the arclength. Then, we can get these geometrical relations of the right ending point (Eq. (1)) and the bending moment at any section along the beam (Eq. (2)) as follows:

$$y_m = \delta \cos \alpha, \quad x_m = L - u = L - \delta \sin \alpha \tag{1}$$

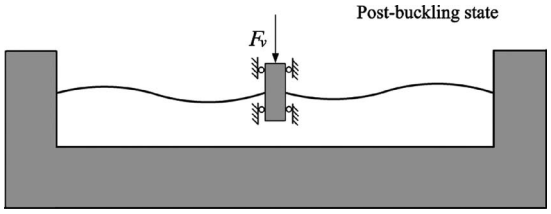

Fig. 2 Post-buckling state of the bent-beam structure

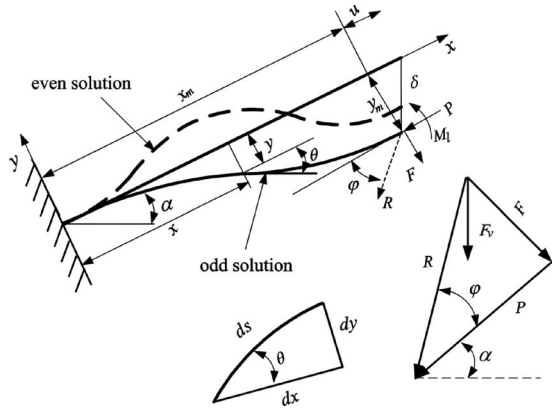

Fig. 3 Deformation of post-buckling beam under a combined load

$$M = -R((y + y_m)\cos \varphi + (x_m - x)\sin \varphi) + M_l \tag{2}$$

Here, δ, x_m, and y_m represent the vertical displacement, longitude deflection, and transverse deflection of the right ending point, respectively. φ is the angle of the elastic force R, θ the angle of any section along the buckled beam, and α the initial angle of the inclined beam. M_0 and M_l stand for the bending moments at the two ending points, respectively. P and F, which can be expressed as $P=R\cos\varphi$ and $F=R\sin\varphi$, are axial and transverse components of the elastic force R, respectively.

Then, from Euler–Bernoulli moment-curvature relationship

$$M = EI\frac{d\theta}{ds} \tag{3}$$

the governing equation of the post-buckling beam with both ends fixed is obtained from Eqs. (2) and (3),

$$\frac{d\theta}{ds} = \frac{-R[(y + y_m)\cos \varphi + (x_m - x)\sin \varphi] + M_l}{EI}$$

$$\frac{dy}{ds} = \sin \theta$$

$$\frac{dx}{ds} = \cos \theta \tag{4}$$

Upon the differentiation of s in Eq. (4), another expression of the governing equation can be obtained as

$$\frac{d^2\theta}{ds^2} = -\frac{R}{EI}(\cos \varphi \sin \theta - \sin \varphi \cos \theta) \tag{5}$$

By integrating θ, the relation between the moment and the elastic force can be derived from Eq. (5) as follows:

$$\frac{R}{EI}(\cos \varphi \cos \theta + \sin \varphi \sin \theta) + c = \frac{1}{2}\left(\frac{M}{EI}\right)^2 \tag{6}$$

where c is the integration constant.

At the inflection point of the deflected beam, where $\theta=\theta^*$, substituting $M=0$ in Eq. (6) results in

$$c = -\frac{R}{EI}\cos(\theta^* - \varphi) \tag{7}$$

The boundary conditions can be written as follows:

$$s = L, \quad \theta = 0, \quad y = -y_m, \quad x = x_m$$

$$s = 0, \quad \theta = 0, \quad y = 0, \quad x = 0 \tag{8}$$

By applying the boundary conditions to Eq. (6), the relation between R and φ is found as follows:

$$c = \frac{1}{2}\left(\frac{M_l}{EI}\right)^2 - \frac{R\cos\varphi}{EI} = \frac{1}{2}\left(\frac{M_0}{EI}\right)^2 - \frac{R\cos\varphi}{EI} \tag{9}$$

Then, the moment at any section of the beam in different buckling modes is obtained by substituting Eq. (7) into Eq. (6),

$$M = \pm\left(\frac{R\cos(\theta - \varphi) - R\cos(\theta^* - \varphi)}{EI}\right)^{1/2} \tag{10}$$

where $\pm$ stands for the direction of the moment.

When the applied vertical force exceeds the critical buckling value, the inclined beam buckles and the second bifurcation of the post-buckling beam occurs. The phenomenon such as snap through, which includes the transition between the asymmetric and the symmetric buckling modes, can be described by the post-buckling analysis.

2.2.1 Asymmetric Mode (Odd Solution). Based on the deflection configuration, which has odd inflection points as shown in Fig. 2, and the concavo-convex relations of the curve, we can

conclude that the directions of the moments at the two ending points of the beam are opposite. Therefore, the relation of the moments on the two ending points of the inclined beam can be obtained from Eq. (9),

$$M_0 = -M_l \tag{11}$$

The moment at the right ending point can be obtained from Eqs. (2) and (11),

$$M_l = \frac{R}{2}(y_m \cos\varphi + x_m \sin\varphi) \tag{12}$$

By substituting Eq. (7) into Eq. (9), the other expression of the moment at the right ending point can be deduced as

$$M_l^2 = 2REI[\cos\varphi - \cos(\theta^* - \varphi)] \tag{13}$$

Upon the substitution of Eq. (12) into Eq. (13), the following relation between θ^* and R can be obtained:

$$\cos(\theta^* - \varphi) = -\frac{R}{8EI}(y_m \cos\varphi + x_m \sin\varphi)^2 + \cos\varphi \tag{14}$$

2.2.2 Symmetric Mode (Even Solution). Based on the deflection configuration, which has even inflection points as shown in Fig. 2, and the symmetry of the beam configuration, we can learn that the moments at the two ending points are in the same direction. So, the moment relation between the two ending points can be deduced from Eq. (9)

$$M_0 = M_l \tag{15}$$

The direction angle φ of the elastic force R can be derived from Eq. (2),

$$\tan\varphi = \frac{F}{P} = -\frac{y_m}{x_m} \tag{16}$$

From Eq. (13), the moment at the right ending point can be written as

$$M_l = [2REI(\cos\varphi - \cos(\theta^* - \varphi))]^{1/2} \tag{17}$$

The condition (Eq. (8)) is self-explanatory and Eq. (1) indicates the fact that the right ending point of the beam can move only in the vertical direction, as shown in Fig. 2. With a given tip displacement δ (controlling parameter) and the three constraint conditions (Eqs. (1), (12), and (17)), the nonlinear differential equation (Eq. (4)) cannot be solved to determine the displacement variables (x,y) and the inclination θ. Therefore, another two constraint conditions are necessary to calculate the elastic force R and its direction angle φ to settle the strong nonlinear statically indeterminate problems.

3 Nonlinear Constraint Conditions of the Postbuckling Beam

3.1 Constraint Condition on the Beam Length. From Eq. (10), the moment-curvature equation of the buckled beam can be written as

$$\frac{d\theta}{ds} = \pm\left(\frac{R\cos(\theta-\varphi) - R\cos(\theta^*-\varphi)}{EI}\right)^{1/2} \tag{18}$$

where the symbol $\pm$ shows the curve direction of the statically indeterminate beam.

Here, set n as the number of the inflection points. When n is odd, the configuration becomes asymmetric; when n is even, the configuration becomes symmetric. The deflection curve can be divided into $2n$ parts by the inflection points and the peak points, and then the constraint condition on the beam length can be obtained by integrating the curved coordinate s in Eq. (18).

Upon substituting the following parameters,

$$\beta = \theta - \varphi, \quad \gamma = \theta^* - \varphi, \quad \sin\frac{\beta}{2} = \sin\frac{\gamma}{2}\sin\phi \tag{19}$$

into Eq. (18), we can get the expression for the beam length.

3.1.1 Asymmetric Modes (Odd Solution). When n is odd, the integration of Eq. (18) results in

$$L = \sqrt{\frac{EI}{2R}}\sum_{k=1}^{2n}\int_{\theta^*\sin([(k-1)/2]\pi)}^{\theta^*\sin(k\pi/2)} \frac{\sin\left(\frac{k+2}{2}\pi\right) - \sin\left(\frac{k+1}{2}\pi\right)}{[\cos(\theta-\varphi) - \cos(\theta^*-\varphi)]^{1/2}}d\theta$$
$$= -2n\sqrt{\frac{EI}{2R}}\int_0^{\theta^*}\frac{d\theta}{[\cos(\theta-\varphi) - \cos(\theta^*-\varphi)]^{1/2}} \tag{20}$$

The constraint condition on the beam length is obtained by substituting Eq. (19) into Eq. (20),

$$L = -2n\sqrt{\frac{EI}{R}}\int_{\phi_0}^{\pi/2}\frac{d\phi}{\left(1-\sin^2\frac{\gamma}{2}\sin^2\phi\right)^{1/2}} \tag{21}$$

When $\theta=0$, from Eq. (19), an expression for Φ_0 can be deduced,

$$\sin\phi_0 = -\frac{\sin(\varphi/2)}{\sin(\gamma/2)} \tag{22}$$

3.1.2 Symmetric Mode (Even Solution). When n is even, the beam length can be calculated by the same method, which has been used in the asymmetric mode.

$$L = \sqrt{\frac{EI}{2R}}\sum_{k=1}^{2n}\int_{\theta^*\sin([(k-1)/2]\pi)}^{\theta^*\sin(k\pi/2)} \frac{\sin\left(\frac{k+2}{2}\pi\right) - \sin\left(\frac{k+1}{2}\pi\right)}{[\cos(\theta-\varphi) - \cos(\theta^*-\varphi)]^{1/2}}d\theta$$
$$= n\sqrt{\frac{EI}{R}}\int_0^{\gamma}\frac{d\beta}{\left(\sin^2\frac{\gamma}{2} - \sin^2\frac{\beta}{2}\right)^{1/2}}$$
$$= 2n\sqrt{\frac{EI}{R}}\int_0^{\pi/2}\frac{d\phi}{\left(1-\sin^2\frac{\gamma}{2}\sin^2\phi\right)^{1/2}} \tag{23}$$

Therefore, by combining Eqs. (21) and (23), the general form of the constraint condition on the beam length can be obtained,

$$L = 2n(-1)^n\sqrt{\frac{EI}{R}}\int_{\phi_0}^{\pi/2}\frac{1}{\left(1-\sin^2\frac{\gamma}{2}\sin^2\phi\right)^{1/2}}d\phi \tag{24}$$

Here, when n is even, Φ_0 is equal to zero; when n is odd, the value of Φ_0 can be determined by Eq. (22).

3.2 Constraint Condition on Displacement. From Eqs. (4) and (18), the displacement (x,y) at any section of the deformed beam can be obtained as follows:

$$x = \int_0^l \cos\theta ds$$

$$y = \int_0^l \sin\theta ds \tag{25}$$

By integrating the equations above, the longitude and transversal displacements (x_m, y_m) of the right ending point can be obtained as follows:

$$x_m = n(-1)^n \sqrt{\frac{2EI}{R}} \int_{\phi_0}^{\pi/2} \frac{\cos(\beta+\varphi)}{\left(1-\sin^2\frac{\gamma}{2}\sin^2\phi\right)^{1/2}} d\phi$$

$$y_m = n(-1)^n \sqrt{\frac{2EI}{R}} \int_{\phi_0}^{\pi/2} \frac{\sin(\beta+\varphi)}{\left(1-\sin^2\frac{\gamma}{2}\sin^2\phi\right)^{1/2}} d\phi \quad (26)$$

Then, the relationship between the longitude and transverse displacements of the right ending point can be simplified as

$$x_m = n(-1)^n \left(\frac{2EI}{R}\right)^{1/2} [I_2 \cos\varphi - I_1 \sin\varphi]$$

$$y_m = n(-1)^n \left(\frac{2EI}{R}\right)^{1/2} [I_1 \cos\varphi + I_2 \sin\varphi] \quad (27)$$

where

$$I_1 = 2\sqrt{2}\sin\frac{\gamma}{2}\int_{\phi_0}^{\pi/2} \sin\phi d\phi = 2\sqrt{2}\sin\frac{\gamma}{2}\cos\phi_0$$

$$I_2 = \sqrt{2}\int_{\phi_0}^{\pi/2} \frac{2\cos^2\frac{\beta}{2}-1}{\left(1-\sin^2\frac{\gamma}{2}\sin^2\phi\right)^{1/2}} d\phi$$

$$= 2\sqrt{2}\int_{\phi_0}^{\pi/2} \left(1-\sin^2\frac{\gamma}{2}\sin^2\phi\right)^{1/2} d\phi - \sqrt{2}\int_{\phi_0}^{\pi/2} \frac{1}{\left(1-\sin^2\frac{\gamma}{2}\sin^2\phi\right)^{1/2}} d\phi$$

When n is odd, the relation between φ and the displacements of the right ending point can be written from Eqs. (14), (19), and (27) as follows:

$$\tan\varphi = \frac{x_m}{y_m} \quad (28)$$

The variables such as φ and R in Eq. (27) are unknowns; so, the displacement constraint relation of the right ending point can be obtained by solving Eq. (27),

$$x_m \cos\varphi - y_m \sin\varphi = 2n\sqrt{\frac{EI}{2R}} I_2 \quad (29)$$

Then, the constraint equation for Eq. (4) can be explicitly found by substituting I_2 into Eq. (29),

$$\frac{1}{L}\int_{\phi_0}^{\pi/2} \frac{d\phi}{\left(1-\sin^2\frac{\gamma}{2}\sin^2\phi\right)^{1/2}} = \frac{2}{x_m\cos\varphi - y_m\sin\varphi + L}\int_{\phi_0}^{\pi/2} \left(1-\sin^2\frac{\gamma}{2}\sin^2\varphi\right)^{1/2} d\varphi \quad (30)$$

The noncomplete elliptic integrals of the first kind can be expressed as the power series to simplify the nonlinear post-buckling governing equation (Eq. (4))

$$\int_0^{\pi/2} \frac{d\phi}{\left(1-\sin^2\frac{\gamma}{2}\sin^2\phi\right)^{1/2}} = \frac{\pi}{2}\left\{1+\sum_{n=1}^{\infty}\left[\frac{(2n-1)!!}{(2n)!!}\right]^2\left(\sin^2\frac{\gamma}{2}\right)^n\right\} \times \int_0^{\phi_0} \frac{d\phi}{\left(1-\sin^2\frac{\gamma}{2}\sin^2\phi\right)^{1/2}}$$

$$= \phi_0 + \sum_{n=1}^{\infty} \frac{(2n-1)!!}{(2n)!!}\left(\sin^2\frac{\gamma}{2}\right)^n \int_0^{\phi_0} \sin^{2n}\phi d\phi \quad (31)$$

where

$$\int_0^{\phi_0} \sin^{2n}\phi d\phi = -\frac{(2n)!}{2^{2n}(n!)^2}\left[\cos\phi_0 \sum_{k=0}^{n-1} \frac{2^{2k}(k!)^2\sin^{2k+1}\phi_0}{(2k+1)!} - \phi_0\right]$$

In other words, with a given displacement δ, the moment M_I can be obtained from Eqs. (12) and (17) and then, the elastic force R and its direction angle φ can be calculated by combining Eqs. (16), (24), (28), and (30). Finally, the strong nonlinear equation (Eq. (4)) can be solved numerically.

4 Analysis of Post-buckling Elastic Force

According to the minimal energy principle, the beam will find the path with the least energy such as the first and second buckling modes in the snap-through process. That is to say, there will be one or two inflection points along the deflection curve of the post-buckling beam under the combined forces.

Based on the geometric relations and force equilibrium relationship, the vertical elastic force F_v can be written as

$$F_v = R(\cos\varphi\sin\alpha + \sin\varphi\cos\alpha) \quad (32)$$

where the elastic force can be expressed as $R=2EI(I_1/L)^2$, which can be calculated from Eqs. (16), (19), (24), and (30). The transversal force F_v is a hidden function of the displacement of the right ending point δ.

When $\cos(\varphi)$ is less than $\cos(\theta^*-\varphi)$, the second bifurcation occurs, and then the buckled beam snaps from the symmetric mode to the asymmetric mode. The formula for calculating φ changes from Eq. (16) to Eq. (28), and the moment expression also changes from Eq. (17) to Eq. (12). Therefore, it is obvious that the snap-through characteristic of the post-buckling beam can be described by the relation between the elastic force and the vertical displacement.

5 Numerical Simulation and Experiments

Based on the theoretical derivation mentioned above, the structure parameters given below are used in simulating the post-buckling behavior of the inclined beam with both ends fixed.

By using the conditions expressed by Eqs. (12), (17), (16), (24), (28), and (30), and a given δ, the variables of M_I, R, and φ can be determined. Now, the modified numerical method of incremental displacement is adopted to solve the governing equation of the post-buckling beam. During the numerical simulation procedure, the variable n mentioned above is found to fulfill the nonlinear constraint conditions on the beam length (as in Eq. (24)). Then, with the inflection point number n, the nonlinear stiffness and the large deflection equilibrium paths during the post-buckling and snap-through process are presented in the following.

To validate the theoretic derivation and the further applications of post-buckling beams, an electronic testing device is designed as shown in Fig. 6, and a series of experiments is conducted to verify the nonlinear stiffness analytically calculated in this paper. As shown in Fig. 6, the post-buckling testing device consists of a

Table 1 Beam parameters

Parameters	Value
Length L	30 mm
Width b	1 mm
Thickness h	0.2 mm
Young's modulus E	160 GPa

displacement sensor, a force sensor, a supporting platform, and two output screens. The inclined Be-bronze beams are fixed on the post-buckling platform when the vertical force is applied to the fixed central point of the structure. When the central point moves vertically, the values of the central point displacement and the corresponding reaction force can be sensed and displayed on the two different screens, respectively. The parameters of the beam structure are identical to those in Table 1.

Figures 4 and 5 show the configurations of post-buckling beams with different initial angles α when the beam tip moves vertically under the applied forces. To facilitate the analytical process, it is necessary to point out that the beam tips shown in both Figs. 4 and 5 correspond to the fixed central point of the testing structure in Fig. 6. When the vertical force applied is zero or less than the critical buckling value, the beam stays in the original state. When the vertical force exceeds the critical buckling value, the beam experiences instability and produces two inflection points, as shown in Figs. 4 and 5. As the vertical displacement of the beam

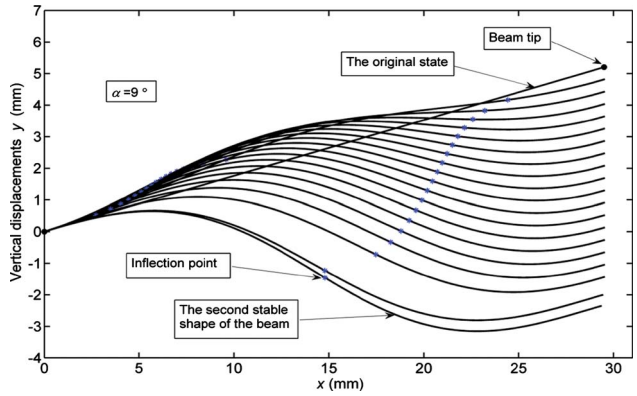

Fig. 4 Post-buckling configurations for α=9 deg

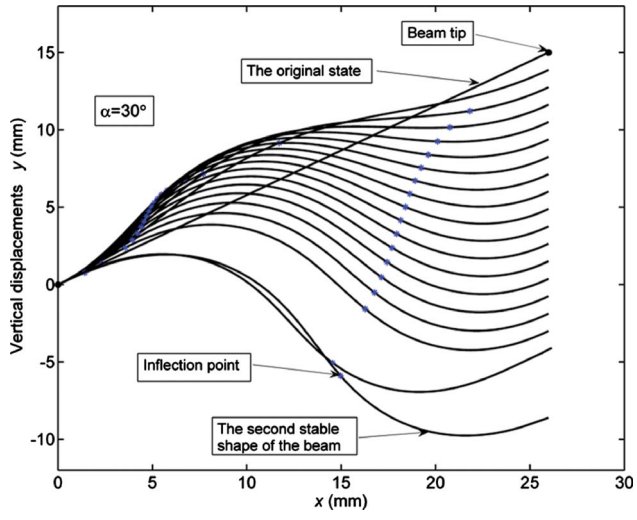

Fig. 5 Post-buckling configurations for α=30 deg

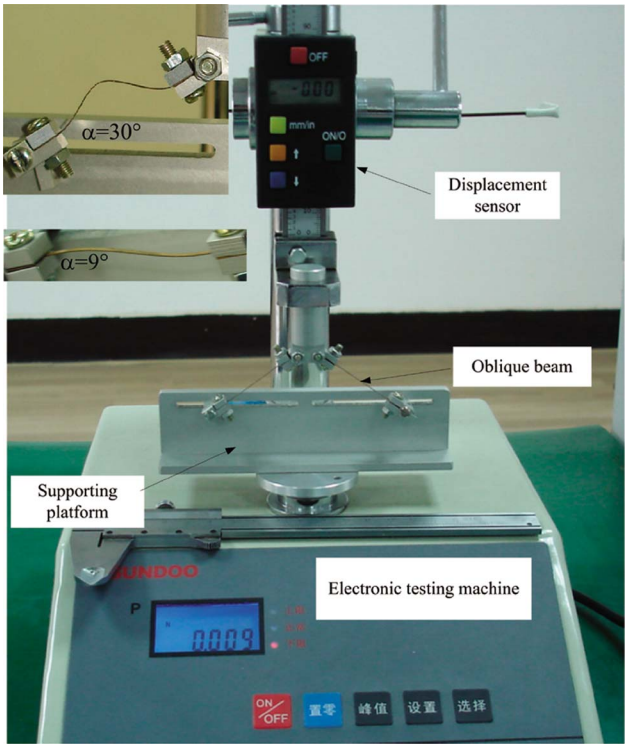

Fig. 6 Electronic testing device for post-buckling beams

tip increases, the configuration of the beam becomes asymmetric; meanwhile, the inflection point number becomes odd correspondingly. These configurations of the post-buckling beams shown in Figs. 3 and 4 are almost the same as those obtained by the experiments.

Figures 7 and 8 show that the simulation results of nonlinear stiffness are in good agreement with those by experiments. In the oxy coordinate system in Figs. 7 and 8, the x axis is the vertical displacement of the beam tip (the central point of the structure) under the applied force. In Figs. 7 and 8, the origin of the x axis stands for the original position of the beam tip, as shown in Figs. 4 and 5. When the applied vertical force F_v exceeds the critical buckling value, the inclined beam will buckle under the compression load, and the elastic force F_v will decrease with the increas-

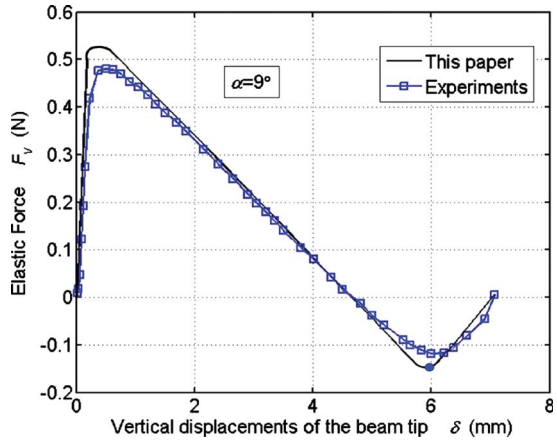

Fig. 7 Elastic force versus displacement for α=9 deg. The filled circle "●" stands for the position where the beam configuration changes from symmetric state to asymmetric state.

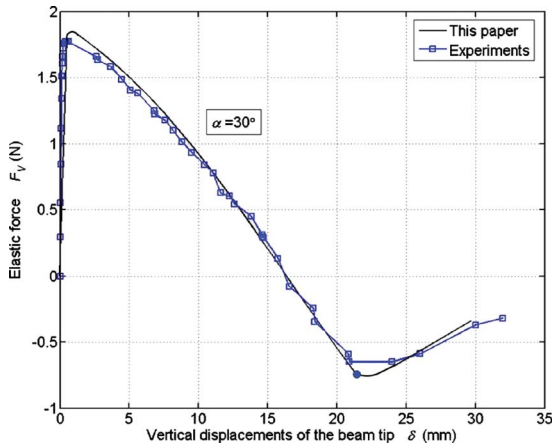

Fig. 8 Elastic force versus displacement for α=30 deg. The filled circle "●" stands for the position where the beam configuration changes from symmetric state to asymmetric state.

ing vertical displacement δ of the beam tip. The elastic force F_v keeps positive until the beam tip approaches a critical unstable position where the elastic force changes to zero. Then, the elastic force becomes negative as the displacement of the beam tip increases, which indicates that the beam will snap to the other stable position automatically. This nonlinear phenomenon of the post-buckling beam is consistent with the results obtained by experiments. The snap-through phenomenon is also depicted in Refs. [12,13]. By regulating the initial angle and dimensions of the post-buckling beams, different forcedisplacement curves can be obtained to fulfill practical applications. Therefore, the post-buckling nonlinear stiffness and the threshold characteristic of the bent beam can be utilized in designing different kinds of threshold accelerometers or other safe-arming systems.

In the special case shown in Fig. 9, when the initial angle equals 90 deg, the configurations obtained in this paper are consistent with the numerical results revealed in Ref. [7]. In Fig. 10, the variation of the axial force with the vertical displacement δ,

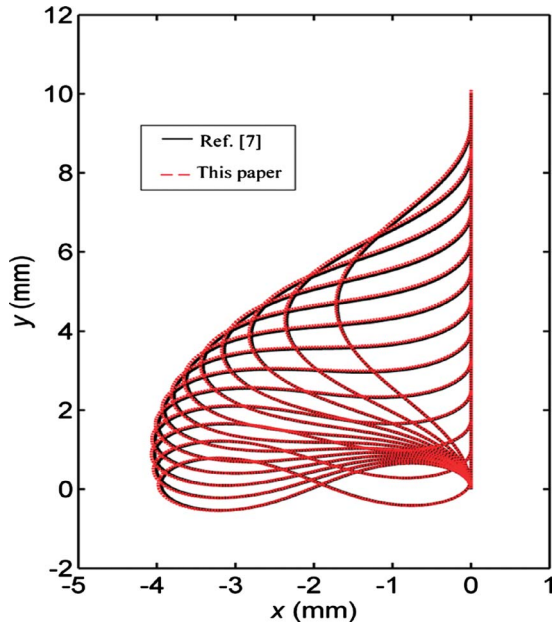

Fig. 9 Large deformation of the beam subjected to axial load for α=90 deg

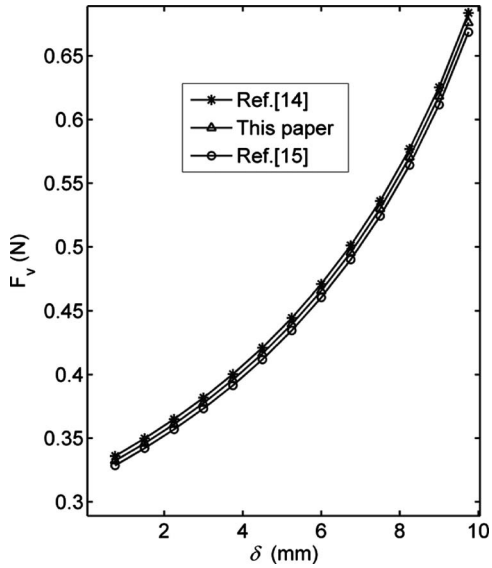

Fig. 10 Force-displacement curve for α=90 deg

which is consistent with the analytical results in Refs. [14,15], shows that the axial load increases with the displacement of the ending point δ. By a comparison of the results between the numerical simulation and the experiments, the analytical method for analyzing post-buckling beams proves feasible in this paper.

6 Conclusion

In order to solve the post-buckling problem and analyze snap-through behavior of the inclined beam with both ends fixed, the governing differential equations of the post-buckling beam subjected to combined forces at the ending point are established. By using an incremental displacement numerical method, the post-buckling configurations of the large deflection beam at any initial inclination angle are presented, and the nonlinear stiffness of the post-buckling beam is obtained in the snap-through process. The numerical results are consistent with those by experiments. Some important conclusions are obtained to find application in optimal design of post-buckling structures.

Moreover, the postbuckled beam snaps from the double-inflection state to the single-inflection state only when the beam experiences large deflections. The high order mode configuration of the buckling beam does not appear in the snap-through process in the static experiments. In addition, the beam under a transversal force does not snap until the beam tip passes a certain unstable position. Furthermore, the critical buckling load increases with an increasing initial angle α, so does the critical displacement. Finally, the incremental displacement numerical method can be used to solve any nonlinear post-buckling problems of inclined beams with large deflection.

Acknowledgment

The authors wish to express their sincere thanks to the NSAF Joint Foundation of China (Grant No. 10476019).

Special gratitude is owed to the two anonymous referees, Ms. Li Wanli and Ms. Ren Lihua, whose comments and suggestions greatly helped us to improve the presentation and quality of the paper.

References

[1] Enikov, E. T., Kedar, S. S., and Lazarov, K. V., 2005, "Analytical Model for Analysis and Design of V-Shaped Thermal Microactuators," J. Microelectromech. Syst., **14**(4), pp. 788–798.

[2] Seide, P., 1975, "Accuracy of Some Numerical Methods for Column Buckling," J. Engrg. Mech. Div., **101**(5), pp. 549–560.

[3] Mau, S. T., 1989, "Buckling and Post-Buckling Analyses of Columns With Discrete Supports," J. Eng. Mech., **115**(3), pp. 721–739.
[4] Fang, W., and Wickert, J. A., 1994, "Post-Buckling of Micromachined Beams," J. Micromech. Microeng., **4**(3), pp. 182–187.
[5] Wang, C. Y., 1997, "Post-Buckling of a Clamped-Simply Supported Elastica," Int. J. Non-Linear Mech., **32**(6), pp. 1115–1122.
[6] Hartono, W., 1997, "Elastic Nonlinear Behavior of Truss System Under Follower and Non-Follower Forces," Comput. Struct., **63**(5), pp. 939–949.
[7] Hartono, W., 2001, "On the Post-Buckling Behavior of Elastic Fixed-End Column With Central Brace," Z. Angew. Math. Mech., **81**(9), pp. 605–611.
[8] Coffin, D. W., and Bloom, F., 1999, "Elastica Solution for the Hygrothermal Buckling of a Beam," Int. J. Non-Linear Mech., **34**(6), pp. 935–947.
[9] Li, S. R., and Zhou, Y. H., 2005, "Post-Buckling of a Hinged-Fixed Beam Under Uniformly Distributed Follower Forces," Mech. Res. Commun., **32**(4), pp. 359–367.
[10] Gianchandani, Y. B., and Najafi, K., 1996, "Bent-Beam Strain Sensors," J. Microelectromech. Syst., **5**(1), pp. 52–58.
[11] Que, L., Park, J. S., and Gianchandani, Y. B., 2001, "Bent-Beam Electrothermal Actuators-Part I: Single Beam and Cascaded Devices," J. Microelectromech. Syst., **10**(2), pp. 247–253.
[12] Qiu, J., Lang, J. H., and Slocum, A. H., 2001, "A Centrally-Clamped Parallel-Beam Bistable MEMS Mechanism," *14th IEEE International Conference on Micro Electro Mechanical System*, IEEE, Switzerland, pp. 353–356.
[13] Jasmina, C. T., and Andrei, S., 2004, "Dynamic Analysis of a Snap-Action Micromechanism," *Conference on IEEE Sensors'04*, Vienna, Austria, pp. 1245–1248.
[14] Timoshenko, S. P., and Gere, J. M., 1988, *Theory of Elastic Stability*, 2nd ed., McGraw-Hill, New York, Chap. 2.
[15] Wang, L. M., and Fan, Q. S., 1996, "Study of Post Buckling Behaviour for the Phase to Phase Composite Spacer," Journal of Tsinghua University (Science and Technology)., **36**(9), pp. 70–76.